



The heat and moisture transfer balance theory of garment simulation[☆]

Ge Lin^{a,b,*}, Siming Meng^{a,b}, Ruomei Wang^{a,c}, Xiaonan Luo^{a,b}, Yi Li^c

^a Institute of Computer Application, Sun Yat-sen University, Guangzhou, 510006, China

^b Engineering Research Center of Digital Life, Ministry of Education, Guangzhou, 510006, China

^c Institute of Textiles and Clothing, Polytechnic University of Hong Kong, Hung Hom, Hong Kong

ARTICLE INFO

Keywords:

Balance theory
Heat and moisture transfer
Grassmann space
Blossom methods
Finite volume methods

ABSTRACT

To establish the human body model to analyze the heat and moisture transfer on body surface, a new explicit definition of rational L-recursion surface is given and the L-recursion surfaces, in Grassmann spaces, are constructed by using blossom method of the homogeneous normal pyramid form. Based on our human body model, the balance theory of garment simulation, the heat and moisture transfer balance equations, called ICAD-balance equations are obtained. The balance theory of garment simulation integrally studies the complex system of human body–fabric–environment. At the same time, the method of obtaining the heat and moisture transfer balance equations is also based on the mass conservation law, the energy conservation law and the Fish law of capillarity. A finite volume method is employed to solve the ICAD-balance equations.

© 2011 Elsevier B.V. All rights reserved.

1. Introduction

Comfortability and aesthetic property are the most important ingredients of influencing consumers to choose garments and the most important ingredients of comfortability includes thermal-wet (heat and moisture transfer), tactile, and pressure [1]. The balance theory of garment simulation [2,3] studies the modeling of the geometric surfaces of human bodies and cloths, and finds their balance (continuity) conditions. In fact, how to obtain the balance equations is the main content of the balance theory. The balance equations are obtained based on some physical laws such as the physical characteristics of fabric, force conditions, the heat transfer (e.g. conduction, convection, radiation, and transform) law, and the moisture transfer (e.g. molecular diffusion, capillary effect, and diffusion of turbulence) law. Balance theory of garment provides a good tool for customized clothing design, electronic mirror for clothing-test-platform, and the research of the comfortable evaluation of cloths.

Since the late 1970s, researchers have realized that the human body, fabric and the environment compose an intrinsic connected system, and heat and moisture transfer balance is the main ingredient of this human body–fabric–environment system. The study of this system has affinitive relationship to the human's comfortability. In this paper, we establish the heat and moisture transfer balance equations, called ICAD-balance equations, based on five assumptions and three basic physical laws. The finite volume method is used to solve the ICAD-balance equations. Both system simulation and experiment results show that ICAD-balance equations can efficiently simulate the reality.

How to construct human body model is an important issue in balance theory of garment simulation. In general, the human body model in garment simulation system is based on space rectangular mesh [4], but it is very difficult to construct

[☆] This work is supported by NSFC Guangdong Joint Fund (U0735001, U0835004, U0935004) and National Key Technology R&D Program of China (No. 2007BAH13B01).

* Corresponding author at: Institute of Computer Application, Sun Yat-sen University, Guangzhou, 510006, China. Tel.: +86 013450433882.

E-mail addresses: 2005.ge.lin@gmail.com (G. Lin), mengsm_zsu@163.com (S. Meng).

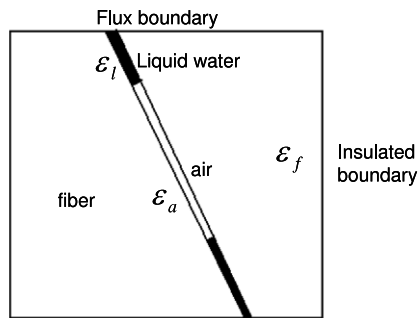


Fig. 1. The structure of fabric and the capillary phenomenon.

and parameterize a space rectangular mesh. The rational L-recurrent surfaces obtained by Blossom method can be used to overcome this difficulty, since the rational L-recurrent surfaces are more flexible in definition and simple in calculation. In Refs. [4–6], with the needs of particular applications, a general definition of recursion surfaces, the so-called L-surfaces, was given. For its application in the balance theory of garment simulation system, this paper gives a new explicit definition of rational L-surface. Then, the blossom method [7,8] is used to produce the L-surface by the normal pyramid form in Grassmann space, where Grassmann space means a linear space formed by the particles and the vectors [9].

2. Heat and moisture transfer balance theory of garment simulation

2.1. Construct the heat and moisture transfer balance equations

One's cloth is just as his/her second layer skin. Therefore, the character of thermodynamics of the cloth is important for his/her feeling of comfort or not. Heat and moisture transfer balance theory discusses the transfer of heat and moisture among human body, fabric and environment. The heat and moisture transfer balance equations are obtained based on the mass conservation law, the energy conservation law and the Fish law of capillarity.

To obtain the heat and moisture transfer balance equations, we assume the following.

The volume of a fabric does not change during absorbing moisture.

The inertia force of liquid water flow is and should be neglected.

The outer air convection (e.g. the wind blow) is and should be neglected.

The cloth is even, i.e., the structure of fiber (e.g. material and sparse holes distribution) and thermodynamic parameters are the same over the cloth.

The times of balancing the heat and moisture between human body and cloth and between cloth and environment are and should be neglected. If the five conditions above are satisfied, according to [10,2,3,11–13], we obtain the balance equations of heat and moisture transfer as follows:

$$\frac{\partial U_a}{\partial t} - \frac{1}{\tau_a} \nabla \cdot (D_a \nabla U_a) = -\xi_1 \epsilon_f \Gamma_f + \epsilon_l \Gamma_{lg}, \quad (1)$$

$$\frac{\partial U_l}{\partial t} - \frac{1}{\tau_l} \nabla \cdot (D_l(\epsilon_l) \nabla U_l) = -\xi_2 \epsilon_f \Gamma_f - \epsilon_l \Gamma_{lg}, \quad (2)$$

$$C_v \frac{\partial T}{\partial t} - \nabla \cdot (K_{mix} \nabla T) = \epsilon_f \Gamma_f (\xi_1 \lambda_v + \xi_2 \lambda_l) - \lambda_{lg} \Gamma_{lg} \quad (3)$$

where $U_a(x, y, z, t) = C_a(x, y, z, t) \epsilon_a$ and $U_l(x, y, z, t) = C_l(x, y, z, t) \epsilon_l$ (See Fig. 1, λ_v is the vapor's heat absorbing or desorbing ratio on the boundary of the capillarity vessel of a fabric, λ_l is the water's heat absorbing or desorbing ratio on the boundary of the capillarity vessel of a fabric).

ξ_1 and ξ_2 are the sorption rates of moisture on the capillarity vessel surface of bounding the water vapor and the liquid water, respectively, i.e., $\xi_1 = \frac{\epsilon_a}{\epsilon}$, $\xi_2 = \frac{\epsilon_f}{\epsilon}$, $\epsilon = \epsilon_a + \epsilon_f$,

Γ_f means the effective sorption rate of the moisture [14], $\Gamma_f = \text{const.} + a_1 C_a + a_2 T$, and

Γ_{lg} is the evaporation (condensation) rate of liquid water (vapor) [14], $\Gamma_{lg} = \frac{\epsilon_a}{\epsilon} h_{lg} S_v (C^*(T) - C_a)$.

2.2. Model's discretization

We use finite volume method to discrete ICAD-balance equations. The solution domain is $\Omega \times \Omega \times \Omega = [0, 1] \times [0, 1] \times [0, 1]$. The x axis means the width, y is the height, and z is the thickness. For convenience, we assume that the space slots in each direction are equal and denoted by h . We also assume that the time slot is Δt . Thus, it has

$$x_i = ih, \quad y_j = jh, \quad z_k = kh, \quad t_l = l\Delta t, \quad 0 \leq i, j, k \leq n, \quad l \geq 0.$$

From Eqs. (1)–(3), we have

$$\int_{vol} \int_t^{t+\Delta t} \frac{\partial U_a}{\partial t} dt dvol = \int_t^{t+\Delta t} \int_{vol} \left\{ \frac{1}{\tau_a} \left[\frac{\partial}{\partial x} \left(\frac{\partial U_a}{\partial x} \right) + \frac{\partial}{\partial y} \left(\frac{\partial U_a}{\partial y} \right) + \frac{\partial}{\partial z} \left(\frac{\partial U_a}{\partial z} \right) \right] - \xi_1 \varepsilon_f \Gamma_f + \varepsilon_l \Gamma_{lg} \right\} dvol dt \quad (4)$$

$$\int_{vol} \int_t^{t+\Delta t} \frac{\partial U_l}{\partial t} dt dvol = \int_t^{t+\Delta t} \int_{vol} \left\{ \frac{1}{\tau_a} \left[\frac{\partial}{\partial x} \left(\frac{\partial U_l}{\partial x} \right) + \frac{\partial}{\partial y} \left(\frac{\partial U_l}{\partial y} \right) + \frac{\partial}{\partial z} \left(\frac{\partial U_l}{\partial z} \right) \right] - \xi_2 \varepsilon_f \Gamma_f + \varepsilon_l \Gamma_{lg} \right\} dvol dt \quad (5)$$

$$\int_{vol} \int_t^{t+\Delta t} \frac{\partial T}{\partial t} dt dvol = \int_t^{t+\Delta t} \int_{vol} \left\{ \frac{1}{C_v} \left[\frac{\partial}{\partial x} \left(K_{mix} \frac{\partial T}{\partial x} \right) + \frac{\partial}{\partial y} \left(K_{mix} \frac{\partial T}{\partial y} \right) + \frac{\partial}{\partial z} \left(K_{mix} \frac{\partial T}{\partial z} \right) \right] + \varepsilon_f \Gamma_f (\xi_1 \lambda_v + \xi_2 \lambda_l) - \lambda_{lg} \Gamma_{lg} \right\} dvol dt \quad (6)$$

The following Eqs. (7)–(9) are the discretization version of Eqs. (4)–(6)

$$\begin{aligned} (U_a)_{ijk}^{l+1} - (U_a)_{ijk}^l &= \Delta t \left\{ \frac{1}{\tau_a} \left[(D_{ax})_{ijk}^{l+1} \left[\frac{(U_a)_{(i+1)jk}^{l+1} - 2(U_a)_{ijk}^l + (U_a)_{(i-1)jk}^{l+1}}{(\Delta x)^2} \right] \right. \right. \\ &\quad + (D_{ay})_{ijk}^{l+1} \left[\frac{(U_a)_{i(j+1)k}^{l+1} - 2(U_a)_{ijk}^l + (U_a)_{i(j-1)k}^{l+1}}{(\Delta y)^2} \right] \\ &\quad + (D_{az})_{ijk}^{l+1} \left[\frac{(U_a)_{ij(k+1)}^{l+1} - 2(U_a)_{ijk}^l + (U_a)_{ij(k-1)}^{l+1}}{(\Delta z)^2} \right] \left. \right] \\ &\quad + [-\xi_1 \varepsilon_f (\Gamma_f)_{ijk}^{l+1} + \varepsilon_l (\Gamma_{lg})_{ijk}^{l+1}] - [-\xi_1 \varepsilon_f (\Gamma_f)_{ijk}^l + \varepsilon_l (\Gamma_{lg})_{ijk}^l] \end{aligned} \quad (7)$$

$$\begin{aligned} (U_l)_{ijk}^{l+1} - (U_l)_{ijk}^l &= \Delta t \left\{ \frac{1}{\tau_a} \left[(D_{lx})_{ijk}^{l+1} \left[\frac{(U_l)_{(i+1)jk}^{l+1} - 2(U_l)_{ijk}^l + (U_l)_{(i-1)jk}^{l+1}}{(\Delta x)^2} \right] \right. \right. \\ &\quad + (D_{ly})_{ijk}^{l+1} \left[\frac{(U_l)_{i(j+1)k}^{l+1} - 2(U_l)_{ijk}^l + (U_l)_{i(j-1)k}^{l+1}}{(\Delta y)^2} \right] \\ &\quad + (D_{lz})_{ijk}^{l+1} \left[\frac{(U_l)_{ij(k+1)}^{l+1} - 2(U_l)_{ijk}^l + (U_l)_{ij(k-1)}^{l+1}}{(\Delta z)^2} \right] \left. \right] \\ &\quad + [-\xi_2 \varepsilon_f (\Gamma_f)_{ijk}^{l+1} + \varepsilon_l (\Gamma_{lg})_{ijk}^{l+1}] - [-\xi_2 \varepsilon_f (\Gamma_f)_{ijk}^l + \varepsilon_l (\Gamma_{lg})_{ijk}^l] \end{aligned} \quad (8)$$

$$\begin{aligned} (T)_{ijk}^{l+1} - (T)_{ijk}^l &= \Delta t \left\{ \frac{1}{C_v} \left[((K_{mix})_x)_{ijk}^{l+1} \left[\frac{(T)_{(i+1)jk}^{l+1} - 2(T)_{ijk}^l + (T)_{(i-1)jk}^{l+1}}{(\Delta x)^2} \right] \right. \right. \\ &\quad + ((K_{mix})_y)_{ijk}^{l+1} \left[\frac{(T)_{i(j+1)k}^{l+1} - 2(T)_{ijk}^l + (T)_{i(j-1)k}^{l+1}}{(\Delta y)^2} \right] \\ &\quad + ((K_{mix})_z)_{ijk}^{l+1} \left[\frac{(T)_{ij(k+1)}^{l+1} - 2(T)_{ijk}^l + (T)_{ij(k-1)}^{l+1}}{(\Delta z)^2} \right] \left. \right] \\ &\quad + [\varepsilon_f (\Gamma_f)_{ijk}^{l+1} (\xi_1 \lambda_v + \xi_2 \lambda_l) - \lambda_{lg} (\Gamma_{lg})_{ijk}^{l+1}] - [\varepsilon_f (\Gamma_f)_{ijk}^l (\xi_1 \lambda_v + \xi_2 \lambda_l) - \lambda_{lg} (\Gamma_{lg})_{ijk}^l]. \end{aligned} \quad (9)$$

Γ_f and Γ_{lg} can be discretized as follows

$$(\Gamma_f)_{ijk}^l = \text{const.} + a_1 (C_a)_{ijk}^l + a_2 (T)_{ijk}^l, \quad (10)$$

$$(\Gamma_{lg})_{ijk}^l = \frac{\varepsilon_a}{\varepsilon} h_{lg} s_v ((C^*(T_{ijk}^{l+1}) - C^*(T_{ijk}^l)) - ((C_a)_{ijk}^{l+1} - (C_a)_{ijk}^l)). \quad (11)$$

3. Use L-surface and its blossom to construct human body models

3.1. The explicit definition of rational L-surface

The definition of rational L-surface was given in Refs. [4–6]. To fit the application in heat and moisture transfer balance theory of garment simulation, we give a new explicit definition of rational L-surface.

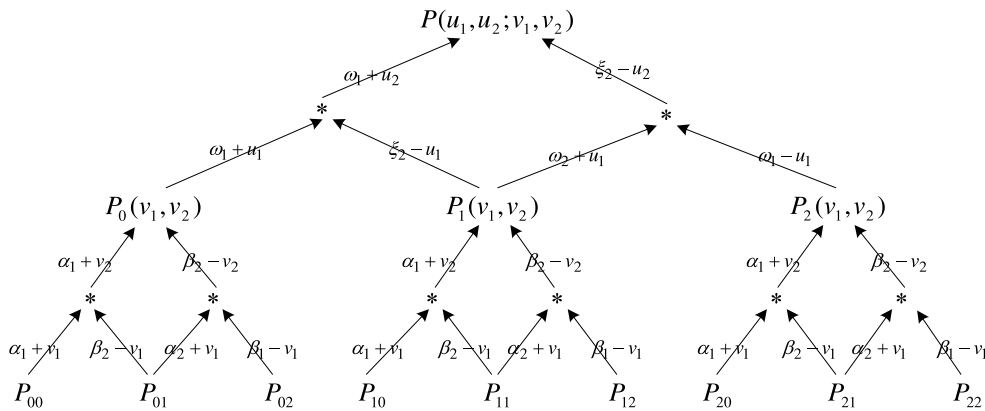


Fig. 2. The recurrence pyramid of 3*3 degree rational L-surface ($\alpha_i + v_j$ means $\frac{\alpha_i + v_j}{\alpha_i + \beta_j}$, $\beta_i + v_j$ means $\frac{\beta_i - v_j}{\alpha_i + \beta_j}$).

Definition 1. Given $(n + 1) * (m + 1)$ points P_{ij} ($i = 0 \dots n, j = 0 \dots m$) in three-dimensional space and the parameters $\alpha_i, \beta_k, \gamma, \omega_j, \xi_l, \varepsilon$ ($i = 0 \dots n - 1, k = i + 1 \dots n, j = 0 \dots m - 1, l = j + 1 \dots m$). Suppose $\gamma\alpha_i + (1 - \gamma)\beta_j \neq 0$ and $\varepsilon\omega_k + (1 - \varepsilon)\xi_l \neq 0$, then the definition of rational L-surface is given by

$$L_{ij}^{k,l}(u, v) = \begin{cases} P_{ij}, & k = 0, l = 0, i = 0 \dots n, j = 0 \dots m, \\ [\lambda_{i,k}(u), \mu_{i,k}(u)] \begin{bmatrix} L_{i,j}^{k-1,l-1}(u, v) & L_{i,j+1}^{k-1,l-1}(u, v) \\ L_{i+1,j}^{k-1,l-1}(u, v) & L_{i+1,j+1}^{k-1,l-1}(u, v) \end{bmatrix} \begin{bmatrix} \phi_{j,l}(v) \\ \varphi_{j,l}(v) \end{bmatrix} \end{cases}$$

$$u, v \in [a, b] \times [c, d], k = 0 \dots n, i = 0 \dots n - k, l = 0 \dots m, j = 0 \dots m - l, \quad (12)$$

where

$$\lambda_{i,k}(u) = \frac{\gamma(\alpha_i + u)}{\gamma\alpha_i + (1 - \gamma)\beta_k}, \quad \mu_{i,k}(u) = \frac{(1 - \gamma)\beta_k - \gamma u}{\gamma\alpha_i + (1 - \gamma)\beta_i},$$

$$\phi_{j,l}(v) = \frac{\varepsilon(\omega_j + v)}{\varepsilon\omega_j + (1 - \varepsilon)\xi_l}, \quad \varphi_{j,l}(v) = \frac{(1 - \varepsilon)\xi_j - \varepsilon v}{\varepsilon\omega_j + (1 - \varepsilon)\xi_l}. \quad (13)$$

It is easy to prove that $\lambda_{i,k}(u) + \mu_{i,k}(u) = \phi_{j,l}(v) + \varphi_{j,l}(v) = 1$.

For simplification, we abbreviate $L_{0,0}^{m,n}(u, v)$ to $L(u, v)$ when no confusion arises.

Definition 2. $L(u, v)$ is called a standard rational L-surface if $\gamma = \varepsilon = \frac{1}{2}$. In this case,

$$\lambda_{i,k}(u) = \frac{\alpha_i + u}{\alpha_i + \beta_k}, \quad \mu_{i,k}(u) = \frac{\beta_k - u}{\alpha_i + \beta_k}, \quad \phi_{j,l}(v) = \frac{\omega_j + v}{\omega_j + \xi_l}, \quad \varphi_{j,l}(v) = \frac{\xi_l - v}{\omega_j + \xi_l}. \quad (14)$$

3.2. The blossom method of rational L-surface in Grassmann space

The blossom method [15] converts a single variable higher-order polynomial to a multivariate lower-order polynomial to simplify the calculation. $L(u, v)$ is a rational L-surface of degree $n \times m$ and the pyramid of blossom is illustrated by Fig. 2.

Theorem 1. The recursion equations of rational L-surface can be written as follows:

$$L(u, v) = \left\{ \left(\frac{\alpha_1 + u}{\alpha_1 + \beta_1}, \frac{\beta_1 - u}{\alpha_1 + \beta_1} \right) \otimes \dots \otimes \left(\frac{\alpha_n + u}{\alpha_n + \beta_n}, \frac{\beta_n - u}{\alpha_n + \beta_n} \right) \right\} \\ \times P \left\{ \left(\frac{\omega_1 + v}{\omega_1 + \xi_1}, \frac{\xi_1 - v}{\omega_1 + \xi_1} \right) \otimes \dots \otimes \left(\frac{\omega_m + v}{\omega_m + \xi_m}, \frac{\xi_m - v}{\omega_m + \xi_m} \right) \right\}^T, \quad (15)$$

where $P = \begin{bmatrix} P_{00} & P_{01} & \dots & P_{0m} \\ P_{10} & P_{11} & \dots & P_{1m} \\ \dots & \dots & \dots & \dots \\ P_{n0} & P_{n1} & \dots & P_{nm} \end{bmatrix}$ and $(a, b) \otimes (c, d) = (ac + ad, bc + bd)$ is the discrete convolution.

We respectively use $\sigma_1, \dots, \sigma_n$ and $\delta_1, \dots, \delta_m$ to substitute u and v to obtain the blossom form of (13) as follows:

$$l(\sigma_1, \dots, \sigma_n; \delta_1, \dots, \delta_m) = \left\{ \left(\frac{\alpha_1 + \sigma_1}{\alpha_1 + \beta_1}, \frac{\beta_1 - \sigma_1}{\alpha_1 + \beta_1} \right) \otimes \dots \otimes \left(\frac{\alpha_n + \sigma_n}{\alpha_n + \beta_n}, \frac{\beta_n - \sigma_n}{\alpha_n + \beta_n} \right) \right\} \\ \times P \left\{ \left(\frac{\omega_1 + \delta_1}{\omega_1 + \xi_1}, \frac{\xi_1 - \delta_1}{\omega_1 + \xi_1} \right) \otimes \dots \otimes \left(\frac{\alpha_m + \delta_m}{\alpha_m + \beta_m}, \frac{\beta_m - \delta_m}{\alpha_m + \beta_m} \right) \right\}^T. \quad (16)$$

3.3. The frequently used surfaces produced from rational L-surfaces

Rational L-surface can be easily used to produce some most commonly used surfaces, such as the Bezier surface, the B-spline surface, and the non-uniform rational spline surface.

Theorem 2. A Bezier surface is a rational L-surface.

Proof. In fact, the Bezier surface can be written as

$$B_{ij}^{k,l}(u, v) = \begin{cases} P_{ij}, & k=0, l=0, i=0 \dots n, j=0 \dots m \\ [u, 1-u] \begin{bmatrix} B_{ij}^{k-1,l-1}(u, v) & B_{i+1,j}^{k-1,l-1}(u, v) \\ B_{i+1,j}^{k-1,l-1}(u, v) & B_{i+1,j+1}^{k-1,l-1}(u, v) \end{bmatrix} \begin{bmatrix} v \\ 1-v \end{bmatrix} \\ u, v \in [a, b] \times [c, d], & i=0 \dots n-k, k=0 \dots n, j=0 \dots m-l, l=0 \dots m \end{cases} \quad (17)$$

According to Definition 1, when $\alpha_i = 0, \beta_k = 1$, we obtain

$$\lambda_{i,k}(u) = \frac{\alpha_i + u}{\alpha_i + \beta_k} = u, \quad \mu_{i,k}(u) = \frac{\beta_k - u}{\alpha_i + \beta_k} = 1 - u. \quad (18)$$

Similarly, when $\omega_j = 0, \xi_l = 1$, we have $\omega_j = v, \xi_l = 1 - v$.

So, the Bezier surface is a rational L-surface.

Similarly, it is easy to prove the following Theorems 3–5.

Theorem 3. A B-spline surface is a rational L-surface.

Theorem 4. A non-uniform B-spline surface is a rational L-surface.

Theorem 5. A Rational non-uniform B-spline surface is a rational L-surface.

4. The initial and boundary conditions of heat and moisture transfer

For insulated boundaries (see Fig. 1), we have

$$D_{ax} \frac{\partial U_a}{\partial x} \Big|_{x=0 \text{ or } x=1} = D_{ay} \frac{\partial U_a}{\partial x} \Big|_{y=0 \text{ or } y=1} = D_{bx} \frac{\partial U_l}{\partial x} \Big|_{x=0 \text{ or } x=1} = D_{by} \frac{\partial U_l}{\partial x} \Big|_{y=0 \text{ or } y=1} = 0 \quad (19)$$

$$(K_{mix})_x \frac{\partial T}{\partial x} \Big|_{x=0 \text{ or } x=1} = (K_{mix})_y \frac{\partial T}{\partial x} \Big|_{y=0 \text{ or } y=1} = 0. \quad (20)$$

And for flux boundaries (see Fig. 1), from [16], we have

$$D_{az} \frac{\partial U_a}{\partial z} \Big|_{z=0} = \frac{\varepsilon_a}{\varepsilon_a + \varepsilon_l} h_v ((C_a)_0 - (C_a)_{env}), \quad D_{az} \frac{\partial U_a}{\partial z} \Big|_{z=1} = \frac{\varepsilon_a}{\varepsilon_a + \varepsilon_l} h_v ((C_a)_1 - (C_a)_{sk}) \quad (21)$$

$$D_{lz} \frac{\partial U_l}{\partial z} \Big|_{z=0} = \frac{\varepsilon_a}{\varepsilon_a + \varepsilon_l} s'_v h_{lg} (C^*(T_0) - (C_a)_0), \quad D_{lz} \frac{\partial U_l}{\partial z} \Big|_{z=1} = \frac{\varepsilon_a}{\varepsilon_a + \varepsilon_l} s'_v h_{lg} (C^*(T_1) - (C_a)_1) \quad (22)$$

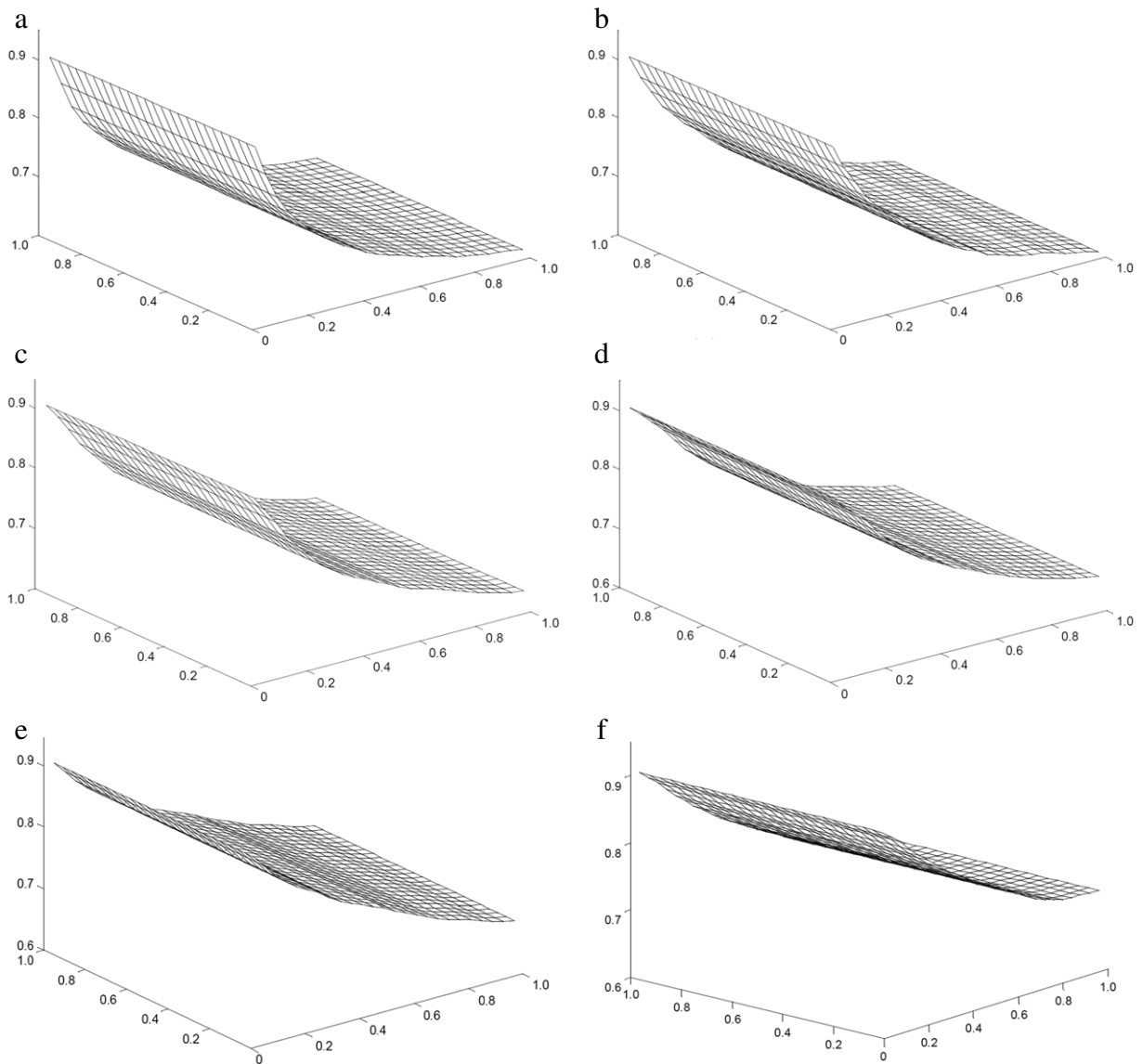
$$(K_{mix})_z \frac{\partial T}{\partial z} \Big|_{z=0} = h_{v0} (T_0 - T_{env}), \quad (K_{mix})_z \frac{\partial T}{\partial z} \Big|_{z=0} = h_{v1} (T_1 - T_{sk}). \quad (23)$$

The initializations of parameters are listed in Table 1.

Table 1

The initializations of parameters [17–19].

Symbol	Physical meaning	Initialization
ρ	Density of the fibers	1.1×10^3
D_f	Diffusion coefficient of water vapor in the fibers of the fabric	5×10^{-13}
θ	Contact angle of the liquid water on the fiber surface	80
ε	Porosity of the fabric	0.90
D_d	Diffusion coefficient of water vapor in the fibers of the fabric	2.5×10^{-5}
γ	Surface tension of liquid water	3×10^3
λ_v	Heat of sorption or desorption of vapor by fibers	2522.0
λ_l	Heat of sorption or desorption of liquid by fibers	2260.0

**Fig. 3.** The simulation of relative humidity change (a) $t = 3$ s, (b) $t = 5$ s, (c) $t = 8$ s, (d) $t = 10$ s, (e) $t = 13$ s, (f) $t = 15$ s.

5. The heat and moisture transfer simulation results

5.1. Simulation in two-dimensional case

According to the ICAD-balance Eqs. (7)–(9), we simulate the transfer processes of heat and water vapor between cloths and human body, respectively lasting 15 s. The simulation results of RH (relative humidity) are shown in Fig. 3. We find that

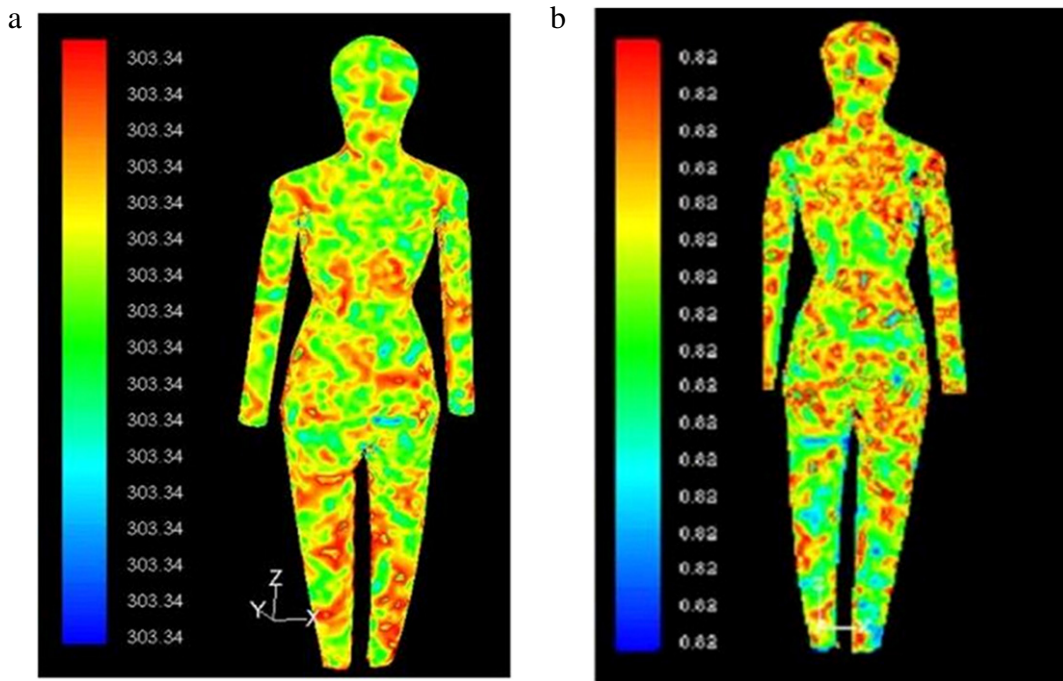


Fig. 4. (a) The temperature distortion, (b) The moisture distortion.

the relative humidity changes faster when the point closing to the human skin. This is the expected result that coincides with our experience.

5.2. The simulation results of human body model

In the SYS-ICAD application system,¹ three-dimensional digital model is used to simulate the heat and moisture transfer process in body–environment–fabric system. The simulation results of the heat and moisture transfer process produced by this system is shown in Fig. 4(a) and (b).

From Fig. 4(a) we found that the heat transfer is not even over all the body. The body surface temperature is between 303.341 and 303.345 K. In fact, our results can reach eight significant digits in the fractional part, but the results shown in Fig. 4(a) and (b) are automatically truncated into three significant digits. Intuitively, it can be seen that yellow, green and red are widely distributed, but the blue ingredient is much less than that of yellow, green and red. The red color represents the temperature of the range [303.3446; 303.34464], the yellow color represents the range [303.34363, 303.34369], and the green color represents the range [303.34277; 303.3428].

Fig. 4(b) shows that the humidity are mainly distributed in the range [0.817433, 0.817490]. Similarly, only three significant digits are shown the figure. In contrast to Fig. 4(a), the distribution of humidity (represented by colors) is mainly composed of red and yellow colors. The red color represents the humidity of the range [0.81748402; 0.81748405] and the yellow color represents the range [0.81747502; 0.81747505]. In fact, these two colors occupy more than 65% of the total body surface, because that skin absorbing water vapor results that the local humidity on the skin is obvious higher than the external. This is consistent with the common sense [1].

6. Conclusion

In this paper, a new explicit definition of rational L-surface is given. And then we use the blossom method to produce the surface in Grassmann space. We prove that the rational L-surface provides a uniform method to construct the Bezier surface, the B-spline surface and the non-uniform B-spline surface. The rational L-surface is used to establish human models to analyze the heat and moisture balance theory in garment simulation. In the heat and moisture transfer balance theory, the laws of mass conservation and energy conservation, and the capillarity are used to obtain the ICAD-balance equations. The ICAD-balance equations are solved by the finite volume method. Both system simulation and experiment results show that the equations can efficiently simulate the reality.

¹ You Fang et al. SYS-ICA Digitized System.

Acknowledgment

We would like to thank Prof. Wang Renhong, Prof. Shi xiquan, Dr. Lin Shujin and Dr. Chen Xiangping for providing us with many good advices on this paper.

References

- [1] Y.Q. Zhong, B.G. Xu, Three-dimensional garment dressing simulation, *Textile Research Journal* 79 (2009) 792–799.
- [2] T. Nishimura, T. Matsuo, Numerical simulation of moisture transmission through a fiber assembly, *Textile Research Journal* 70 (2) (2000) 103–107.
- [3] Z. Wang, Y. Li, Y.L. Kowk, et al., Mathematical simulation of the perception of fabric thermal and moisture sensations, *Textile Research Journal* 72 (4) (2002) 327–334.
- [4] R.M. Wang, Y. Li, F. You, X.N. Luo, Rational recurrence curves and recurrence surfaces in multivariate B-form on some regions, *Journal of Computational and Applied Mathematic* 163 (2004) 277–285.
- [5] Wang RenHong, *Multivariate Spline Functions and their Applications*, Kluwer Academic Publishers, 2001.
- [6] R.M. Wang, X.N. Luo, Y. Li, Representation and conversion of Bezier surfaces in multivariate B-form, *Journal of Computational and Applied Mathematics* 195 (1–2) (2006) 206–211.
- [7] X.N. Luo, H. Nie, Y. Li, Zh.X. Luo, Recurrence surfaces on arbitrary quadrilateral mesh, *Journal of Computational and Applied Mathematics* 144 (2002) 221–232.
- [8] R. Goldman, G. Morin, The affine invariant analytic blossom, *Computer Aided Geometric Design* 19 (2002) 621–623.
- [9] Zh.X. Luo, F.Zh. Li, Y.X. Liu, Y. Li, Effect of the environmental atmosphere on heat, water and gas transfer within hygroscopic fabrics, *Journal of Computational and Applied Mathematics* 163 (1) (2004) 199–210.
- [10] X.N. Luo, S.J. Lin, Recursive curves and surfaces in Grassmann space for computer modeling and animation, in: *Technologies for E-Learning and Digital Entertainment*, in: LNCS, vol. 3942, 2006, pp. 1085–1089.
- [11] X.N. Luo, H.M. Luo, A computing model of pressure distribution from tight underwear, *Journal of Computational and Applied Mathematics* 195 (11) (2006) 106–112.
- [12] X.N. Luo, Q.Zh. Xu, A new numerical implementation on 2D heat and moisture transfer through fabric, *Applied Mathematics and Computation* 174 (2) (2006) 1135–1150.
- [13] J.H. Huang, Y.B. Chen, Effects of air temperature, relative humidity, and wind speed on water vapor transmission rate of fabrics, *Textile Research Journal* 80 (2010) 395–402.
- [14] Y. Li, F.Zh. Li, Q.Y. Zhu, Numerical simulation of virus discussion in facemask during breathing cycles, *International Journal of Heat and Moisture Transfer* 48 (20) (2005) 4229–4242.
- [15] R. Goldman, Blossoming with cancellation, *Computer Aided Geometric Design* 16 (1999) 671–689.
- [16] Z. Wang, Y. Li, C.Y. Yeung, Mathematical simulation of thermal and moisture sensations of knitted fabrics, *Textile Research Journal* 72 (4) (2002) 327–334.
- [17] P.M. Lo Re, D. Olanda, Grassmann spaces, *Journal of Geometry* 17 (1981) 50–60.
- [18] Y. Li, A.H. Mao, R.M. Wang, X.N. Lou, Z. Wang, W.B. Hou, L.Y. Zhou, Y.B. Lin, P-smart—a virtual system for clothing thermal functional design, *Computer-Aided Design* 38 (7) (2006) 726–739.
- [19] R. Goldenthal, Efficient simulation of inextensible cloth, *ACM Transactions on Graphics* 26 (3) (2007) Article 49.